Journal of Advanced Zoology
ISSN: 0253-7214
Volume 45 Issue 01 Year 2024 Page 95:105

Experimental Analysis Of Rotor Blade In Wind Turbine Using Composite Materials With Natural Fiber

M. Siry Chandana[1]*, Dr. K. Kalyani Radha[2]

[1]*PG Scholar, Dept. of Mechanical Engineering, JNTUA College of Engineering Ananthapuramu, Jawaharlal Nehru Technological University Anantapur, Andhra Pradesh 515002, India,
Email: msirychandana@gmail.com
[2]Associate Professor, Dept. of Mechanical Engineering, JNTUA College of Engineering Ananthapuramu, Jawaharlal Nehru Technological University Anantapur, Andhra Pradesh 515002, India,
Email: radha.mech@jntua.ac.in

***Corresponding Author:** - M. Siry Chandana
*PG Scholar, Dept. of Mechanical Engineering, JNTUA College of Engineering Ananthapuramu, Jawaharlal Nehru Technological University Anantapur, Andhra Pradesh 515002, India, Email: msirychandana@gmail.com

Abstract

Rotor blades are a critical structural component of the tidal turbine since they are responsible for harvesting the kinetic energy of the water and transmitting it through the main drive train to the generator. At hand the rotor blades are manufactured using the materials like Conventional Steels and Aluminium Alloys. With the use of these existing materials it results in relatively low fracture toughness in high strength conditions, limited performance at elevated temperature. One of the main drawback of steel is suspected to corrosion and it also loses its properties at high temperatures. To overcome this issue Composite Material is being used. Rotor blade is made up of composite materials. The materials are glass fiber epoxy and natural fiber(sugar cane fiber) with the composition 10% of natural fiber and 90% of glass fiber epoxy. The modeling of the Rotor blade is carried out in SOLID WORKS and analysed using ANSYS FLUENT, Also the rotor blade is fabricated by HAND LAY-UP METHOD. The mechanical properties are tested. The results are validated.

Keywords: E-Glass Fiber, Sugarcane Fiber, Solid works, Ansys Workbench, CFD, Epoxy Resin

1.INTRODUCTION

Wind turbines, designed for the extraction of wind energy, find application in the generation of wind power. A turbine, featuring fan blades, is situated atop a tall tower. The tower's height is strategically chosen to capture higher-speed winds, avoiding hindrances like hills, trees, and structures. When the wind turbine initiates its rotational motion, the generator activates, leading to the generation of electricity. The power output of an individual wind turbine ranges from a few kilowatts for residential purposes to exceeding 5 megawatts for industrial use. Wind turbines are broadly classified into two types: horizontal axis and vertical axis. To ensure that the manufactured turbine blades meet design specifications, each prototype undergoes rigorous experimental testing. These tests involve assessments of fundamental dynamic properties such as natural frequencies and damping, along with evaluations of load-bearing capacity under extreme conditions and resistance to fatigue. Such examinations are pivotal for understanding the overall dynamic behavior and

ensuring the structural integrity of the wind turbine, particularly in relation to properties such as the first torsional mode and the lowest 3–4 flexural bending modes.

1.1 BLADE PROFILE

Airfoils represent aerodynamically efficient profiles capable of producing greater lift than flat plates of equivalent area, while also generating lift with substantially reduced drag. They find extensive application in the development of aircraft, propellers, rotor blades, wind turbines, and various other areas within aeronautical engineering.The fundamental element in designing wind turbine blades is the airfoil, and as a result, enhancing its design is a critical factor in enhancing the aerodynamic efficiency, noise reduction, and structural durability of a rotor blade.

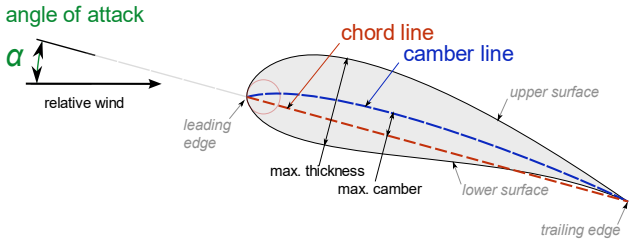

Fig.1.Blade Profile

1.2 SELECTION OF AIRFOIL

The NACA 63-215 series is used for developing the rotor blade.This airfoil is characterized by its distinctive numerical designation, which provides information about its shape.The numbers "63-215" correspond to the airfoil's geometric properties.The NACA 63-215 airfoil was likely developed for specific aerodynamic characteristics, and engineers and researchers would use it based on their requirements for lift, drag, and other performance factors in various applications, such as aircraft wings, wind turbine blades, and other aerodynamic structures. It's important to note that there are many different NACA airfoil designs, each with its own unique performance characteristics.

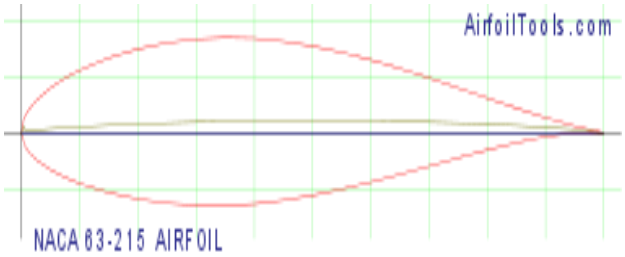

Fig.2.NACA 63-215 Airfoil

2. LITERATURE SURVEY:

Pabut ,O et al [1], Analyzing the structure and operational effectiveness of wind turbine blades is crucial for both the theoretical foundation and practical implementation of wind turbines. Manufacturing costs associated with the blades of a small horizontal axis wind turbine (SHAWT) can make up around 20% of the overall production expenses of the turbine. Therefore, enhancing potential profits involves developing an improved structural model and selecting suitable composite materials through a multifaceted approach that includes multi-criteria optimization and sophisticated modeling techniques.

Arvind Singh Rathore, et al [2], The central objective of this investigation was the enhancement of the rotor design for a 750 kW horizontal axis wind turbine, with a specific emphasis on the crucial component, the blades. The chosen blade, with a length of 21.0 meters, incorporated the S809 airfoil consistently applied from the root to the tip. The study employed the Type Approval Provision Scheme TAPS-2000 as its design methodology. In this framework, all loads induced by wind and inertia on the blades were transmitted to the hub. To assess stress and deflection on both the blades and the hub, the Finite Element Analysis (FEA) method was applied. Following this, the outcomes derived from ANSYS were juxtaposed with the existing design to gauge the efficacy of the proposed optimization.

3. MATERIALS SELECTION FOR ROTOR BLADE:

Sugarcane Fiber/ Bagasse fiber:
Sugarcane fiber is derived from the fibrous residue left behind after sugarcane stalks have their juice extracted. It is considered as lignocellulosic material, primarily composed of cellulose, hemicellulose, and lignin, which form the majority of its structure.Sugarcane fiber is a versatile and eco-friendly reinforcing material known for its strength, stiffness, low weight, and sustainability. The mechanical properties are enhanced by using it in the composite materials but also aligns with the growing emphasis on sustainable and renewable resources in various industries.

Table 1: Material properties of Steel,GFRP,GFRP with Sugarcane

Material Property	Structural Steel	GFRP	GFRP WITH SUGARCANE FIBER
Density(kg/m^3)	7850	2100	1700
Poisson's Ratio	0.3	0.21	0.206
Young's Modulus of Elasticity(GPa)	200	75	38.25

3.1 Epoxy Resin (LY-556): Bisphenol-A diglycidyl ether ($C_{12}H_{24}O_4$) is another name for it. The actual resin is composed of epichlorohydrin and biphenyl (of which there are several types).A common form of biphenyl is created by combining acetone and phenol. When cured, epoxy resins(LY-556), exhibit "rigid but tough bond lines and excellent adhesion to metals," as noted by adhesives.org. Table 2 illustrates the specific characteristics of Epoxy Resin LY-556. This resin establishes a strong bond with natural fibers.

Table 2:Properties of EPOXY RESIN(LY-556)

S.No.	Parameter	Value
1	Modulus of elasticity	25 – 30Gpa
2	Poisson's ratio	0.33
3	Elongation	2 – 4%
4	Shear modulus	1.25Gpa

Fig.3.Epoxy resin LY556

3.2 Hardener (HY-951): $C_6H_{18}N_4$,Hardener is a curing agent for epoxy or fiberglass A hardener, also referred to as a catalyst, is essential for initiating the curing process of epoxy resin or fiberglass. When combined with

resin, it facilitates the solidification of the adhesive. The selection and combination of a specific hardener and epoxy components play a crucial role in determining the final properties and suitability of the epoxy coating for a given environment.

Table 3: Properties of HARDENER (HY-951):

S.No.	Parameter	Value
1	Appearance	Reddish Brown
2	Colour	Colourless
3	Amine value	310 – 350mgKOH/g
4	Viscosity 25°C	3000cPs(max)
5	Density 25°C	0.98 – 1.00gm/cm^3
6	Flash point	81ºC

Fig.4.HARDENER (HY-951)

3.3 E-Glass Fiber:E-glass fiber weighing 700gsm is a specialized reinforcement material employed in composite manufacturing. The elevated weight signifies a more concentrated arrangement of fibers, resulting in heightened strength and stiffness. Selection of this material is contingent upon the application's specific needs and the targeted mechanical properties for the ultimate composite product.

Table 4: Properties of E-GLASS FIBER (700GSM) :

S.No.	Parameter	Value
1	Modulus of elasticity	75Gpa
2	Poisson’s ratio	0.25
3	Temperature	550 °C
4	Density	2.55 g/cm³

Fig.5. E-GLASS FIBER (700GSM)

4. MODELLING OF ROTOR BLADE

The model of the rotor blade is developed by using SOLIDWORKS in the version 22.

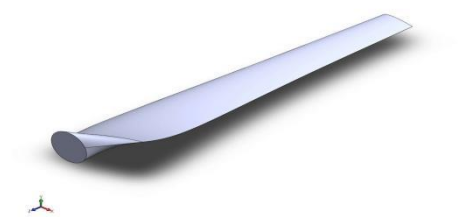

Fig.6.Rotor blade model in SOLIDWORKS

5. STATIC STRUCTURAL ANALYSIS OF ROTOR BLADE:

Meshing: Meshing is the process where the original geometry of rotor blade is discretized into a mesh composed of simple geometric elements such as triangles, quadrilaterals(in 2D) or tetrahedra, hexahedra (in 3D). It is generated using ANSYS 19.2 software.

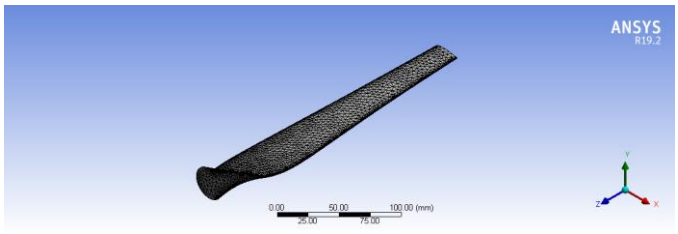

Fig.7.Meshing of the rotor blade using ANSYS

Boundary conditions chosen for the analysis:

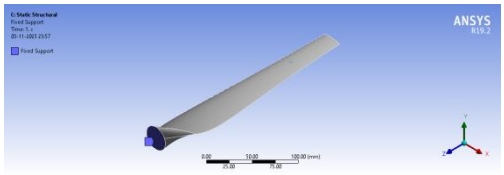

Fig.8.Fixed Support

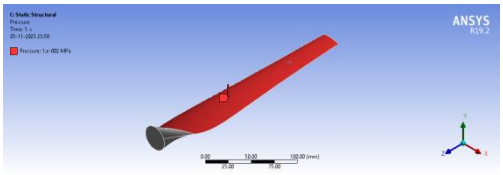

Fig.9.Pressure

The above figures are the boundary conditions given for the rotor blade. The fixed support is given to rotor as shown in the fig 8 and the pressure 0.01MPa is applied above the blade.

6. CFD ANALYSIS OF ROTOR BLADE:

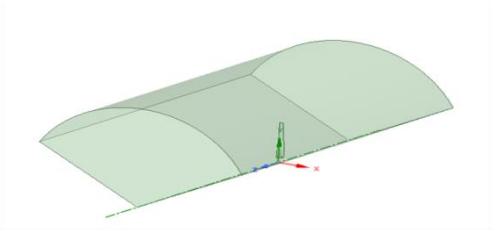

Fig.10.Designing the enclosure of Rotor blade

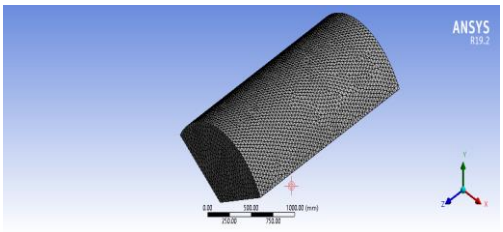

Fig.11.Meshing of the Rotor blade

The model is imported and it is kept in a enclosure as shown in the above figure. Then Boolean operation is done (i.e. subtract). The meshing is done to the enclosure. The solid is given the named selections such as inlet, outlet, blade for convenience. Now open the setup and select the double precision and click on start. In General, solver type is selected as Pressure-Based, velocity is taken as absolute and time is taken as transient.
In models, standard k-omega is chosen to model near blade wall interactions more accurately. In materials air is chosen. Then, Boundary conditions are applied as inlet, velocity inlet magnitude is given as 12m\s in the Z-direction. Then the calculation is initialized using Initialization option. Then under calculations activities, Run Calculation is selected and the results are obtained.

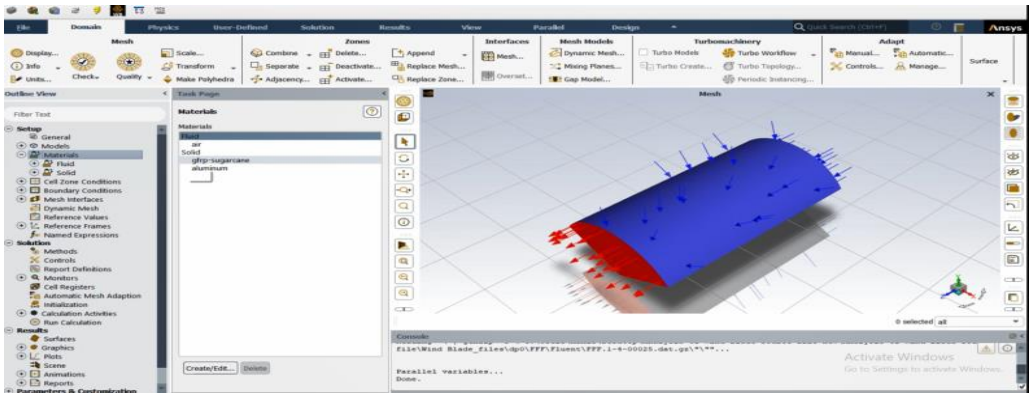

Fig.12.Running Calculations

7. EXPERIMENTAL PROCEDURE: The composite material is prepared by using hand lay-up method The hand lay-up process, which entails layering resin and reinforcing fibers by hand onto a mold, is used to fabricate composite material of the rotor blade. This cost-effective method allows for customization, ensuring precise fiber orientation through skilled labor. The resulting rotor blade fulfill specific automotive requirements, providing advantages in terms of strength, durability, and weight. For experimental testing, the specimen is sliced in accordance with ASTM standards.

Fig.13.Laminated Specimen

8. RESULTS AND DISCUSSIONS

Results of static structural analysis:

Total Deformation:

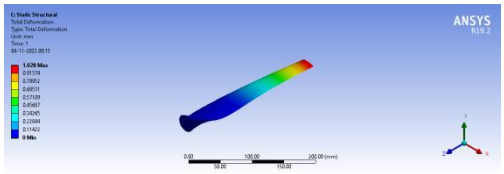

Fig.14.Total deformation of structural steel

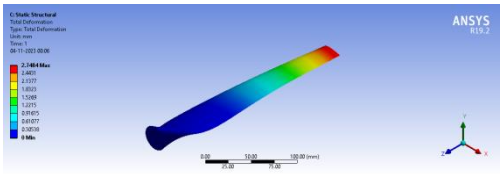

Fig.15.Total deformation of GFRP

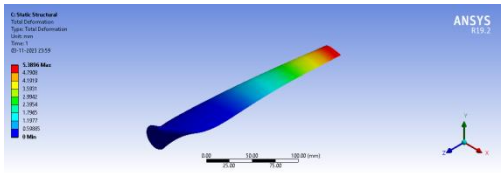

Fig.16.Total deformation of GFRP with Sugarcane

Equivalent stress:

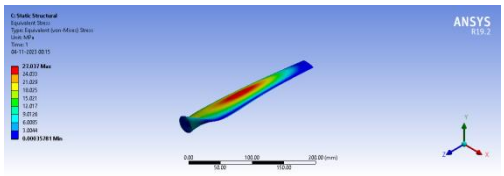

Fig.17.Equivalent stress of structural steel

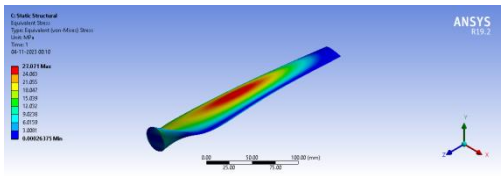

Fig.18.Equivalent stress of GFRP

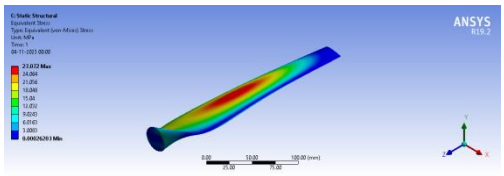

Fig.19.Equivalent stress of GFRP with Sugarcane

Equivalent elastic strain:

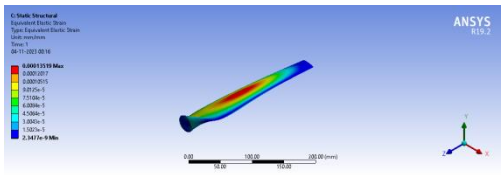

Fig.20.Equivalent elastic strain of structural steel

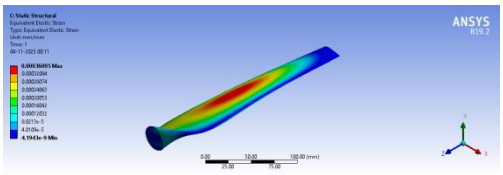

Fig.21.Equivalent elastic strain of GFRP

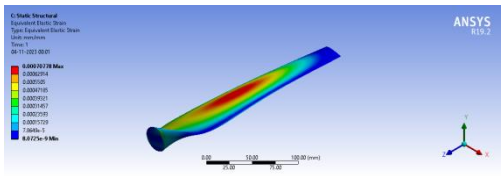

Fig.22.Equivalent elastic strain of GFRP with Sugarcane

Table 5: Comparison of Structural Steel, GFRP, GFRP with Sugarcane fiber

Properties	**Structural Steel**	**GFRP**	**GFRP with Sugarcane fiber**
Density(kg/m^3)	7850	2100	1700
Pressure (MPa)	0.01	0.01	0.01
Young's Modulus of Elasticity(GPa)	200	75	38.25
Total Deformation(mm)	1.028	2.7484	5.3896
Equivalent Stress(MPa)	27.037	27.071	27.072
Equivalent Elastic Strain	0.00013519	0.00036095	0.00070778

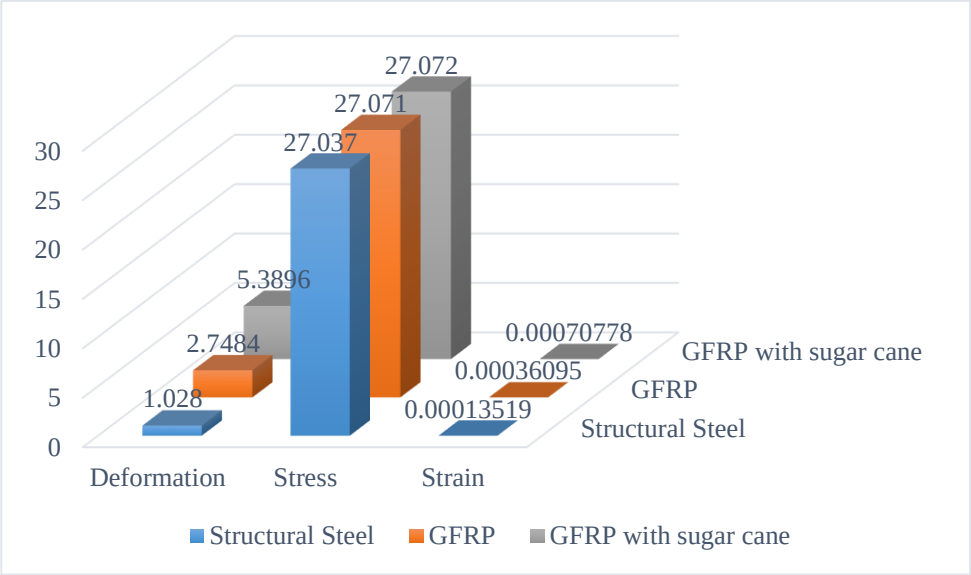

Fig.26.Comparison between materials based on Deformation, Stress, Strain

CFD Analysis Results:

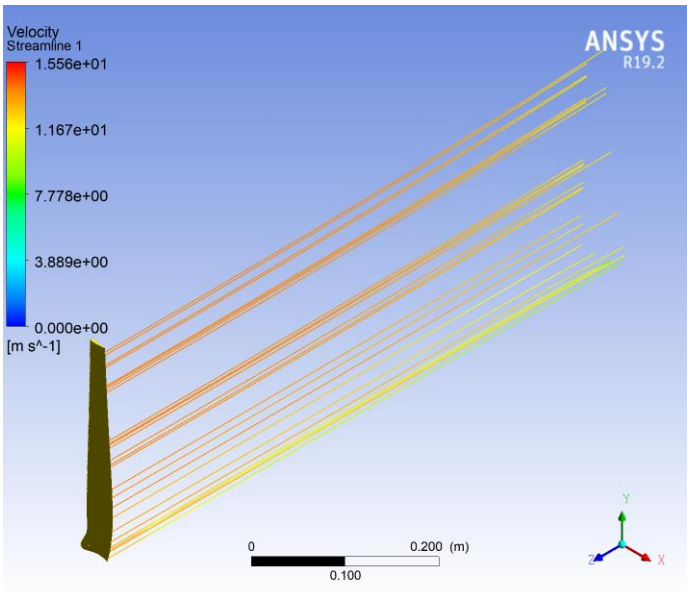

Fig.27.Velocity Streamline

9. EXPERIMENTAL TESTING

From the laminated composites, the specimens are prepared as per ASTM standards and are tested to evaluate their Mechanical Properties like tensile, compression and impact strength. The results by conducting these tests are mentioned below.

MECHANICAL PROPERTIES

A) Tensile Test: ASTM D3039

In the research work, the specimen is tested using universal testing machine. The result of the ultimate tensile load, ultimate tensile strength is calculated and listed in below table.

Table 6: Tensile test results

TEST PARAMETERS	OBSERVED VALUES
Gauge Width (mm)	24.78
Gauge Thickness (mm)	3.39
Original Cross Sectional Area (mm^2)	84.00
Ultimate Tensile Load (KN)	29.13
Ultimate Tensile Strength (N/mm2 or MPa)	347.00

B) Compression Test: ASTM D642

In the research work, the specimen is tested using universal testing machine. The result of the compression load, compression strength is calculated and listed in below table.

Table 7: Compression test results

TEST PARAMETERS	OBSERVED VALUES
Gauge Width (mm)	25.29
Gauge Thickness (mm)	4.24
Original Cross Sectional Area (mm^2)	107.23
Compression Tensile Load (KN)	0.62
Compression Strength (N/mm^2 or MPa)	6.00

C)Impact Strength: ASTM D760-06
In the research work, the specimen is tested using the charpy impact testing machine. The result of charpy impact test includes the amount of energy required to rupture the specimen and corresponding impact strength is calculated and listed in below table.

Table 8: Impact strength test results

Specimen Size	Notch Type	Test Temperature	Absorbed Energy-Joules			Average
			ID-1	ID-2	ID-3	
5 x 13 x 80	Un Notched	+24° C	38	32	22	30.67

Table 9: Experimental Comparison between steel, GFRP, GFRP with Sugarcane fiber

Parameter	Density	Tensile	Compression	Charpy
Structural Steel	7850 kg/m^3	295 MPa	3.5 MPa	24.5 J/cm
GFRP	2100 kg/m^3	303 MPa	5.63MPa	27.88 J/cm
GFRP with Sugarcane	1700 kg/m^3	347 MPa	6 MPa	30.67J/cm

10. CONCLUSION:

It includes modelling of the rotor blade, static structural analysis ,CFD Analysis and experimental testing for the rotor blade.

Total Deformation: GFRP with Sugarcane results the highest total deformation of 5.3896 mm compared to Structural Steel (1.0280 mm) and GFRP (2.7484 mm).This indicates that GFRP with Sugarcane can withstand higher loads without experiencing permanent deformation, making it a suitable material for the rotor blade.
Equivalent stress: GFRP with Sugarcane results a high equivalent stress of 27.072 MPa, which is higher than Structural Steel (27.037 MPa) and GFRP (27.071 MPa). This suggests that GFRP with Sugarcane has high strength and can handle significant stress without failure, further supporting its suitability for the rotor blade.
Equivalent elastic strain: The equivalent elastic strain of GFRP with Sugarcane is 0.00070778, which is higher than that of Structural Steel (0.00013519) and GFRP (0.00036095). This indicates that GFRP with Sugarcane

can withstand higher strains without undergoing plastic deformation, making it a desirable material for the rotor blade.

GFRP with Sugarcane has maximum values in mechanical testing, It has good mechanical properties. The experimental study included making rotor blade prototypes out of glass fibre reinforced polymer (GFRP) reinforced with sugarcane. The mechanical properties and performance of the laminate were tested using tensile, compression, and impact techniques. Compressive testing determined the material's compressive strength and modulus, whereas tensile tests measured its tensile strength, modulus. The impact resistance of the laminate was tested. Understanding the behaviour of the windmill rotor blade required a combination of FEA analysis and experimental inquiry. The validity and veracity of the numerical model might be determined by comparing the FEA analysis findings to the experimental data.

11. REFERENCES

[1] Pabut, Ott & Allikas, Georg & Herranen, Henrik & Talalaev, Robert. (2012). Model Validation and Structural Analysis of a Small Wind Turbine Blade.

[2] Singh Rathore, Arvind & Ahmed, Siraj. (2011). Design and Analysis of Horizontal Axis Wind Turbine Rotor. International Journal of Engineering Science and Technology. 3.

[3] S. Rehman, M. Mahbub Alam, L. M. Alhems, and M. Mujahid Rafique, "Horizontal Axis Wind Turbine Blade Design Methodologies for Efficiency Enhancement A Review," Energies, vol. 11, no. 3, 2018.

[4] U. Fernandez-Gamiz, E. Zulueta, A. Boyano, J. A. Ramos-Hernanz, and J. M. Lopez-Guede, "Microtab design and implementation on a 5MW wind turbine," Appl. Sci., vol. 7, no. 6, 2017.

[5] C. Pavese, C. Tibaldi, F. Zahle, and T. Kim, "Aeroelastic multidisciplinary design optimization of a swept wind turbine blade," Wind Energy, vol. 20, no. 12, pp. 1941–1953, 2017.

[6] P. A. C. Rocha, H. H. B. Rocha, F. O. M. Carneiro, M. E. V. da Silva, and C. F. de Andrade, "A case study on the calibration of the k-ω SST (shear stress transport) turbulence model for small scale wind turbines designed with cambered and symmetrical airfoils," Energy, vol. 97, pp. 144–150, 2016.

[7] W. Hu, K. K. Choi, and H. Cho, "Reliability-based design optimization of wind turbine blades for fatigue life under dynamic wind load uncertainty," Struct. Multidiscip. Optim., vol. 54, no. 4, pp. 953–970, 2016.

[8] P. S. Premkumar et al., "Uncertainty and Risk Assessment in the Design Process for Wind," J. Adv. Res. Dyn. Control Syst., vol. 9, no. February, p. V07AT30A013, 2015.

[9] W. Han, P. Yan, W. Han, and Y. He, "Design of wind turbines with shroud and lobed ejectors for efficient utilization of low-grade wind energy," Energy, vol. 89, pp. 687–701, 2015.

[10] Jha, K., Yeswanth, I.V.S., Manish, D., Tyagi, Y.K. (2021). Structural and Modal Analysis of PEEK-CF Composite for Aircraft Wing. In: Parey, A., Kumar, R., Singh, M. (eds) Recent Trends in Engineering Design. Lecture Notes in Mechanical Engineering. Springer, Singapore. https://doi.org/10.1007/978-981-16-1079-0_12

[11] Global Wind Report (GWEC). Available online: **http://www.gwec.net/wp-content/uploads/vip/GWEC_PRstats2016_EN_WEB.pdf** (accessed on 11 January 2018).

[12] Wind Turbine Schematic. Available online: **http://www.delahyde.com/lubang/imagesl_2013/Wind_Turbine_Schematic_M.jpg** (accessed on 11 January 2018).

[13] Tsai, K.; Pan, C.; Cooperman, A.M.; Johnson, S.J.; Dam, C.P. Van An Innovative Design of a Microtab Deployment Mechanism for Active Aerodynamic Load Control. *Energies* **2015**, *8*, 5885–5897. [**Google Scholar**] [**CrossRef**]

[14] KACARE White Paper. Available online: **https://www.kacare.gov.sa/en/FutureEnergy/RenewableEnergy/Pages/default.aspx** (accessed on 11 January 2018).

[15] Elsevier BV. Scopus Journal Analyzer. 2014. Available online: **http://www.scopus.com/source/eval.url** (accessed on 11 January 2018).

[16] Zheng, Q.; Rehman, S.; Alam, M.; Alhems, L.M.; Lashin, A. Decomposition of wind speed fluctuations at different time scales. *J. Earth Syst. Sci.* **2017**, *126*. [**Google Scholar**] [**CrossRef**]

[17]Rehman, S.; Khan, S. Fuzzy Logic Based Multi-Criteria Wind Turbine Selection Strategy—A Case Study of Qassim, Saudi Arabia. *Energies* **2016**, *9*, 872. [**Google Scholar**] [**CrossRef**]

[18] Shoaib, M.; Siddiqui, I.; Rehman, S.; Rehman, S.; Khan, S.; Lashin, A. Comparison of Wind Energy Generation Using the Maximum Entropy Principle and the Weibull Distribution Function. *Energies* **2016**, *9*, 842. [**Google Scholar**] [**CrossRef**]

[19] Mohandes, M.; Rehman, S.; Abido, M.; Badran, S. Convertible wind energy based on predicted wind speed at hub-height. *Energy Sources Part A Recover. Util. Environ. Eff.* **2016**, *38*, 140–148. [**Google Scholar**] [**CrossRef**]
[20] Khan, S.A.; Rehman, S. Iterative non-deterministic algorithms in on-shore wind farm design: A brief survey. *Renew. Sustain. Energy Rev.* **2013**, *19*, 370–384. [**Google Scholar**] [**CrossRef**]
[21] Bassyouni, M.; Gutub, S.; Javaid, U.; Awais, M.; Rehman, S.; Abdel-Hamid, S.; Abdel-Aziz, M.; Abouel-Kasem, A.; Shafeek, H. Assessment and analysis of wind power resource using weibull parameters. *Energy Explor. Exploit.* **2015**, *33*, 105–122. [**Google Scholar**] [**CrossRef**]
[22] Baseer, M.A.; Meyer, J.P.; Alam, M.M.; Rehman, S. Wind speed and power characteristics for Jubail industrial city, Saudi Arabia. *Renew. Sustain. Energy Rev.* **2015**, *52*, 1193–1204. [**Google Scholar**] [**CrossRef**]
[23] Proietti, S.; Sdringola, P.; Castellani, F.; Astolfi, D.; Vuillermoz, E. On the contribution of renewable energies for feeding a high altitude Smart Mini Grid. *Appl. Energy* **2017**, *185*, 1694–1701. [**Google Scholar**] [**CrossRef**]
[24] Rehman, S.; Sahin, A.Z. A wind-solar PV hybrid power system with battery backup for water pumping in remote localities. *Int. J. Green Energy* **2016**, *13*, 1075–1083. [**Google Scholar**] [**CrossRef**]
[25] Ur Rehman, S.; Rehman, S.; Qazi, M.U.; Shoaib, M.; Lashin, A. Feasibility study of hybrid energy system for off-grid rural electrification in southern Pakistan. *Energy Explor. Exploit.* **2016**, *34*, 468–482. [**Google Scholar**] [**CrossRef**]